JOURNAL OF SOLID STATE CHEMISTRY 53, 193–216 (1984)

Crystal Chemistry and Magnetic Properties of Layered Metal Oxides Possessing the K_2NiF_4 or Related Structures*

P. GANGULY AND C. N. R. RAO†

Solid State and Structural Chemistry Unit, Indian Institute of Science, Bangalore-560012, India

Received June 30, 1983; in revised form January 20, 1984

There is increasing interest in recent years in the structural chemistry and properties of layered metal oxides possessing the K_2NiF_4 or related structures. Many new oxides of this structure exhibiting novel properties are being reported from time to time in the literature. The crystal chemistry of the oxides of the general formula A_2BO_4 with particular reference to the stability of the K_2NiF_4 structure and the relations between the different structures exhibited by this family of oxides is discussed. Non-stoichiometry in these oxides is another aspect of interest discussed in the article. While K_2NiF_4 itself is a well-known two-dimensional antiferromagnet, oxides of this structure with a variety of magnetic properties are examined in some detail. Besides the ternary A_2BO_4 oxides, the structure and magnetic properties of complex oxides, where the A or/and the B ions are partly substituted by other cations, is discussed. Some of the problems related to this family of oxides that are worth investigating are indicated. Much of the discussion in this article would have relevance in understanding the structure and properties of layered materials.

1. Introduction

K_2NiF_4 is a prototype, two-dimensional antiferromagnetic material (*1*). The tetragonal K_2NiF_4 structure consists of alternating layers of $KNiF_3$ perovskite layers and KF rock-salt layers. Antiferromagnetic interactions between the transition metal ions occur only in the planes containing the $KNiF_3$ perovskite layers. There is no Ni–F–Ni interaction in the direction parallel to the c axis. A variety of oxides are known to crystallize in structures related to K_2NiF_4 (*2–14*). Besides the tetragonal K_2NiF_4 structure, A_2BO_4 type oxides with monoclinic, orthorhombic, and other tetragonal structures have been characterized in recent years (*6–9, 13–15*). The main objective of this article is to examine the stability of the K_2NiF_4 structure and the relations between the different structures of metal oxides in this family and to rationalize their properties in terms of the structures. We have discussed at length, the crystal chemistry of various oxides of the A_2BO_4 type in terms of the nature of A–O and B–O bonding and the consequences of the bonding on the structure and properties of the oxides. Non-stoichiometry in these oxides has also been discussed briefly.

Oxides with K_2NiF_4 or related structures exhibit interesting magnetic and electronic

* Contribution No. 213 from the Solid State and Structural Chemistry Unit.

† To whom all correspondence should be addressed at: Department of Physical Chemistry, University of Cambridge, Cambridge, CB2 1EP, United Kingdom.

0022-4596/84 $3.00

properties. It was reported a few years ago (*2*) that La_2NiO_4 shows an activated electrical conductivity behavior at low temperatures, but the resistivity has a positive temperature coefficient above 550 K. Such a semiconductor–metal transition is indeed of great interest. La_2CuO_4 is reported to exhibit a temperature-independent electrical resistivity ($\sim 10^{-1}$ ohm cm), but other rare earth derivatives of the general formula Ln_2CuO_4 are semiconductors (*2*). Electron transport properties of more complex oxides of the K_2NiF_4 family such as $LaSr_3Co_2O_8$ are quite different from those of the corresponding perovskite oxides.

Magnetic properties of oxides possessing K_2NiF_4 structure have been investigated more extensively than electron transport properties. Some of the oxides such as Ca_2MnO_4 show long-range antiferromagnetic ordering while others such as La_2NiO_4 do not. Ferromagnetism is known to occur in oxides such as $LaSr_3Co_2O_8$. The K_2NiF_4 structure appears to preferentially stabilize certain spin states of transitional metal ions and accordingly, some of the transition metal oxides of this family exhibit spin-state transitions. We shall discuss magnetic properties of a variety of oxides possessing K_2NiF_4 type structure in the light of their crystal chemistry.

2. Crystal Chemistry

Compounds of the general formula A_2BX_4 with the K_2NiF_4 structure (Fig. 1) may be considered to be built up of alternating layers of perovskite (ABX_3) and rock-salt (AX) structures. There are no close-packed A_2X_4 layers in A_2BX_4 similar to the close-packed AX_3 layers (Fig. 2a) present in perovskites. In a close-packed A_2X_4 layer, there would be considerable electrostatic repulsion between the two A ions since they are forced to be adjacent to each other if the perovskite AX_3 layers are to be retained within the structure (see Fig. 2b).

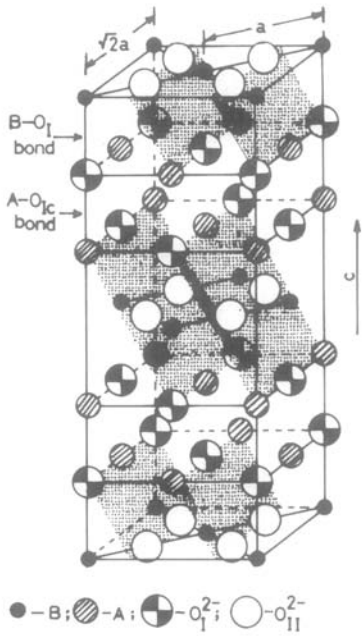

FIG. 1. The K_2NiF_4 structure of A_2BO_4 oxides showing O_I and O_{II} ions. B–O_I and A–O_{Ic} bonds are also shown. Shaded portion shows close-packed AO_3 layers.

The two AX_3 layers can, however, be displaced (Fig. 2c) to give alternating layers of rock-salt and perovskite structures. It is evident from Fig. 1 that along the {110} planes

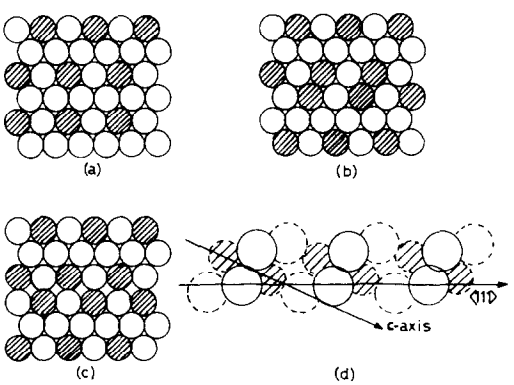

FIG. 2. (a) AX_3 close-packing: hatched circles are A ions and open circles are X ions; (b) hypothetical A_2X_4 close-packing built up from AX_3 layers; (c) displacement of AX_3 layers to give A_2X_4 packing as found in the ideal K_2NiF_4 structures; (d) corrugated packing of A_2X_4 layers as in La_2NiO_4.

of the K_2NiF_4 structure, the {110} planes of the perovskite layers are stacked alternately with the {100} planes of the rock-salt layer. In order to obtain the A_2X_4 packing shown in Fig. 2c, the {111} planes of the perovskite layer should be coplanar with the {100} planes of the rock-salt layer. This is roughly what is achieved along the {111} planes of the K_2NiF_4 structure (see Figs. 1 and 2d), the two planes being corrugated instead of being coplanar. This results in a better packing efficiency. The low c/a ratio (3.25–3.30) found in several A_2BO_4 oxides (compared to the theoretical value of 3.414 ($c = (2 + \sqrt{2})a$) if the BO_6 octahedra were regular and the A–O distances were identical) is perhaps due to the corrugated nature of the packing in the {111} planes. The perovskite (AX_3) layers (Fig. 3a) are displaced in the K_2NiF_4 structure as represented in Fig. 3b. Structures of the related Ruddlesdon–Popper type compounds of the general formula $AX(ABX_3)_n$ with $n = 2$ and 3 are shown in Figs. 3c and d where 2 and 3 layers of perovskites are displaced, respectively. Insertion of an AX layer in the $n = 2$ case (Fig. 3c) between the two perovskite bilayers and a reshuffling of the perovskite layers could give rise to the hypothetical compound $(AX)_2(ABX_3)_2$ with alternating bilayers of rock-salt and perovskite (Fig. 3e) instead of the monolayers found in the K_2NiF_4 structure. We shall discuss later why such compounds are not readily formed.

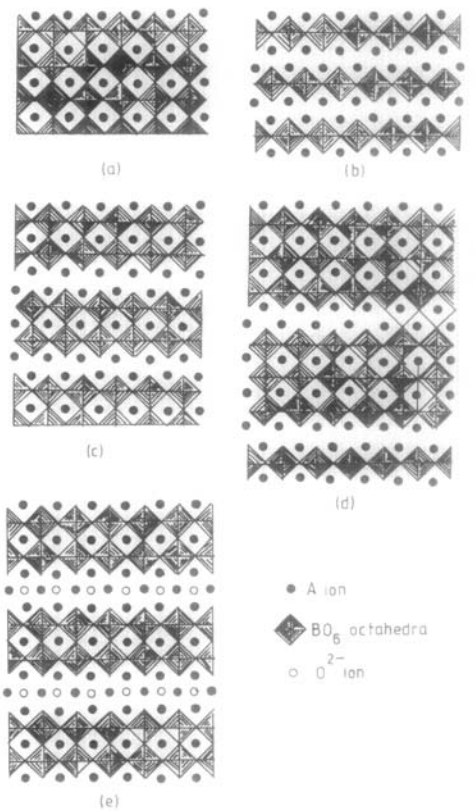

FIG. 3. Projection drawings of (a) ABO_3 perovskites and (b) A_2BO_4 oxides with K_2NiF_4 structure. Projection drawings of $n = 2$ and $n = 3$ members of the series $AO(ABO_3)_n$ are shown in (c) and (d). Projection drawing of hypothetical $(AO)_2(ABO_3)_2$ is shown in (e). After Tilley, Ref. (*45*).

2.1. Stability of the K_2NiF_4 structure in oxides. Just as for perovskite oxides, a tolerance factor t may be defined for A_2BO_4 oxides as

$$t = \frac{r(A\text{–O})}{\sqrt{2}r(B\text{–O})} \qquad (1)$$

Here, $r(A$–O) and $r(B$–O) are distances obtained from ionic radii. Poix (*3*) has defined the tolerance factor for oxides as

$$t = \psi_A/\sqrt{2}\,\beta_B \qquad (2)$$

where ψ_A and β_B are invariant values (*3, 4*) associated with B–O and A–O distances in six- and ninefold coordinations, respectively. The tetragonal K_2NiF_4 structure is assumed to be stable (*3*) within the limits $1.02 > t > 0.85$. This criterion is conceptually more appealing than Ganguli's criterion (*5*) according to which the tetragonal structure is stable when r_A/r_B is between the limits 2.4 and 1.7 when one employs the ionic radii of Shannon (*16*). Such a criterion in terms of A–O and B–O distances is indeed equivalent to Poix's criterion. In this article, we shall adopt Poix's criterion while examining the stability of the tetragonal

structure. We have calculated t and ψ_A for various oxides by using the following relationship proposed by Poix (*3*):

$$\beta_B + \sqrt{2}\,\psi_A = 0.996V^{1/3} \qquad (3)$$

where V is the volume of the unit cell and β_B is available in the literature (*4*). In Table I, we have listed the values of t thus obtained for several compounds. We note that t values of La_2NiO_4, La_2CuO_4, and La_2CoO_4 are close to the lower limit. The orthorhombic structure (*6–8*) of La_2CoO_4 and La_2CuO_4 and the tetragronal structure (*6*) of La_2NiO_4 would seem to be consistent with β_{Ni} being less than β_{Cu} or β_{Co}. The monoclinic distortion in Nd_2NiO_4 and Pr_2NiO_4 (*9*) can be attributed to the low tolerance factor in these two oxides.

In compounds where t is close to the lower limit of stability of the tetragonal K_2NiF_4 structure, it is possible to increase t by several possible mechanisms. In compounds of the type La_2BO_4, β_B can be reduced by the incorporation of a small proportion of B^{3+} ions. Thus, La_2NiO_4 possessing the tetragonal structure almost always contains a finite proportion of Ni^{3+} ions. Low β_B can also arise if the B ions are in the low-spin state instead of in the high-spin state. In Sm_2CoO_4, there is crystal structure evidence (*8*) for two different environments for the Co^{2+} ions.

Investigations on polycrystalline as well as single crystal samples (*6, 10, 11*) of La_2NiO_4 have established the structure of this oxide to be tetragonal. Indeed, it was the first oxide to be shown to have the K_2NiF_4 structure. Recently (*12*), supercells corresponding to $\sqrt{2}\,a$ unit cells (with crystals grown from a skull melter) have been observed in the electron diffraction patterns. Subsequently, it has been found that electron diffraction patterns of La_2NiO_4 prepared by the ceramic method also show such superlattice reflections. These reflections are similar to those in the neutron diffraction pattern of three-dimensional, antiferromagnetically ordered K_2NiF_4. Such superlattice reflections are also observed in La_2CuO_4. Compounds such as La_4LiBO_8 which have similar tolerance factors show superlattice reflections similar to those observed in La_2NiO_4. In Fig. 4a we show electron diffraction patterns corresponding to the tetragonal [111] zone axis of La_4LiCoO_8 and to the tetragonal [110] zone axis of La_2NiO_4 (Fig. 4b) as well as of La_4LiCoO_8 (Fig. 4c). Such superlattice reflections have not been seen in the case of other $LaSrBO_4$ compounds including $La_2Sr_2NiTiO_8$; these oxides have higher tolerance factors. The superlattice reflections may be associated with two different envi-

TABLE I

LATTICE PARAMETERS, $\psi_{Ln^{3+}}$ AND t VALUES FOR SOME OXIDES WITH K_2NiF_4 STRUCTURE

Compounds	a (Å)	c (Å)	c/a	$\psi_{Ln^{3+}}$	t
$LaSrAlO_4$[a]	3.761	12.649	3.363	2.586	0.978
$LaSrVO_4$	3.87	12.65	3.270	2.563	0.914
$LaSrCrO_4$	3.85	12.50	3.25	2.549	0.928
$LaSrMnO_4$	3.804	13.10	3.44	2.537	0.901
$LaSrFeO_4$[b]	3.88	12.76	3.29	2.602	0.922
$LaSrCoO_4$	3.806	12.503	3.285	2.626	0.989
$LaSrNiO_4$	3.80	12.51	3.292	2.521	0.935
La_2CoO_4	3.896[c]	12.66	3.249	2.561	0.852
La_2NiO_4	3.855	12.652	3.282	2.558	0.867
La_2CuO_4	3.807[c]	13.17	3.459	2.53	0.834
$La_2Li_{0.5}Co_{0.5}O_4$[d]	3.784	12.624	3.336	2.519	0.861
$La_2Li_{0.5}Ni_{0.5}O_4$[d]	3.756	12.87	3.426	2.54	0.877
$PrSrAlO_4$	3.732	12.54	3.36	2.523	0.966
$PrSrCrO_4$	3.836	12.377	3.226	2.485	0.909
$PrSrFeO_4$	3.838	12.597	3.282	2.511	0.906
Pr_2NiO_4	3.845[c]	12.44	3.235	2.53	0.857
$NdSrAlO_4$	3.726	12.49	3.352	2.504	0.963
$NdSrCrO_4$	3.834	12.36	3.223	2.501	0.919
$NdSrMnO_4$	3.768	12.98	3.445	2.461	0.888
$NdSrFeO_4$	3.846	12.594	3.274	2.521	0.908
$NdSrNiO_4$	3.786	12.26	3.238	2.448	0.922
Nd_2NiO_4	3.810	12.31	3.231	2.491	0.844
$GdSrAlO_4$[a]	3.701	12.362	3.340	2.442	0.952
$GdSrCrO_4$	3.823	12.263	3.207	2.442	0.902
$GdSrMnO_4$	3.754	12.87	3.428	2.418	0.881
$GdSrFeO_4$	3.853	12.554	3.258	2.523	0.908
$GdSrNiO_4$	3.768	12.23	3.245	2.416	0.916
Gd_2CuO_4	3.89	11.85	3.046	2.452	0.806

[a] Based on the present study.
[b] Lattice parameter data from Ref. (*54*).
[c] Pseudo-tetragonal lattice parameters.
[d] Lattice parameter data from Ref. (*25*). Rest of the lattice parameter data from Ref. (*35, 36*).

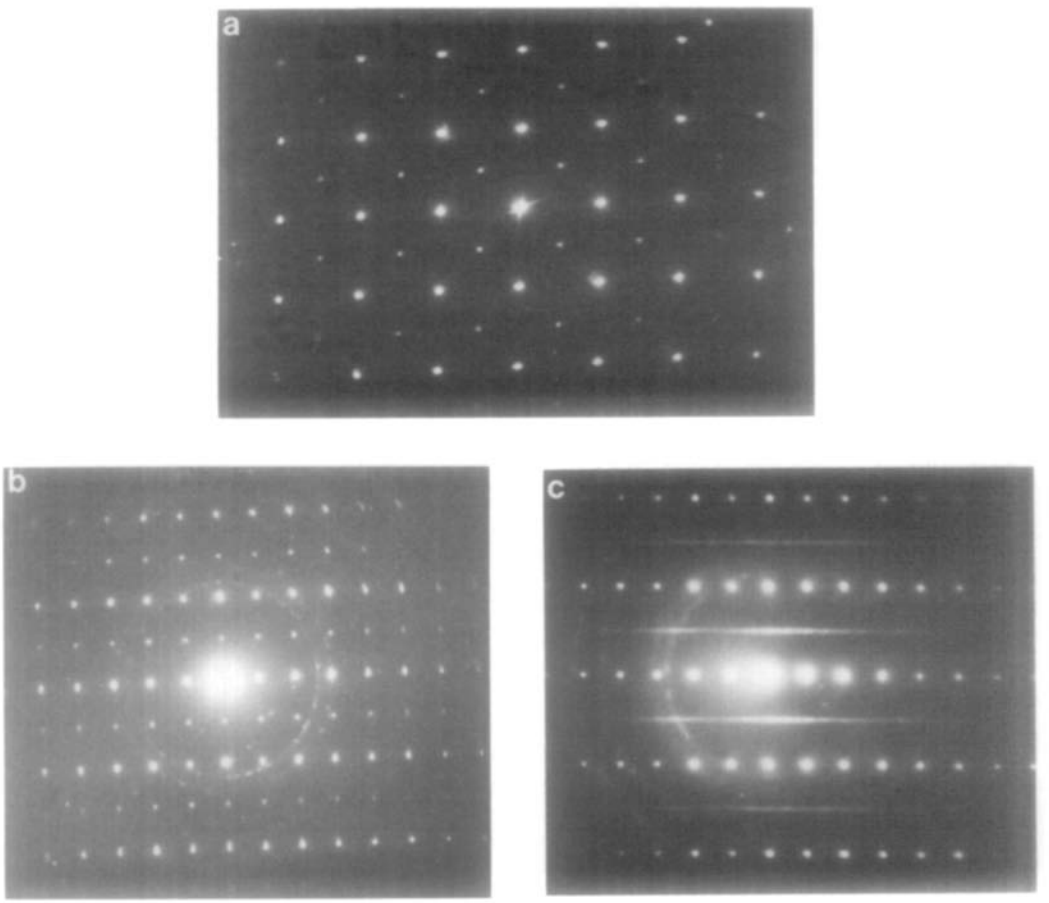

FIG. 4. Electron diffraction patterns corresponding to (a) the [111] zone axis of La_4LiCoO_8, (b) [110] zone axis of La_2NiO_4, and (c) [110] zone axis of La_4LiCoO_8.

ronments of the *B* ions arising from the deviation of the B–O_{II}–B angle from 180° or from changes in the *B*–O distance. The former can happen if $t \approx 0.85$ and the BO_6 octahedra get rotated about the *c* axis (Fig. 5a) or if the octahedra are tilted in the ⟨100⟩ or the ⟨110⟩ directions (Figs. 5b and c). The latter is likely to happen in compounds such as La_4LiBO_8 where the nature of Li–O and *B*–O bonds is quite different. The distortions (and hence the superlattice reflections) in many of the K_2NiF_4 related compounds may be similar to those depicted in Fig. 5.

Several structures can result from a rearrangement of the oxygen ion positions in the K_2NiF_4 structure. Three of these arise from monoclinic distortions with $\gamma \neq 90°$. Of these, there are two structures with $a = b$ which can be indexed on the basis of a orthorhombic unit cell; two types of orthorhombic structures *O* and *O'* have been distinguished (*13*). For the *O* structure, the conditions for the allowed reflections are $h + k = 2n$, $k + l = 2n$ and $h + l = 2n$ while for the *O'* structure, the condition is $k + l = 2n$. In the *O'* structure (*8, 13, 14*) found in La_2CuO_4, La_2CoO_4, and CaY CrO_4, the BO_6 octahedra are tilted as in Fig. 5c. The *O* structure was established for

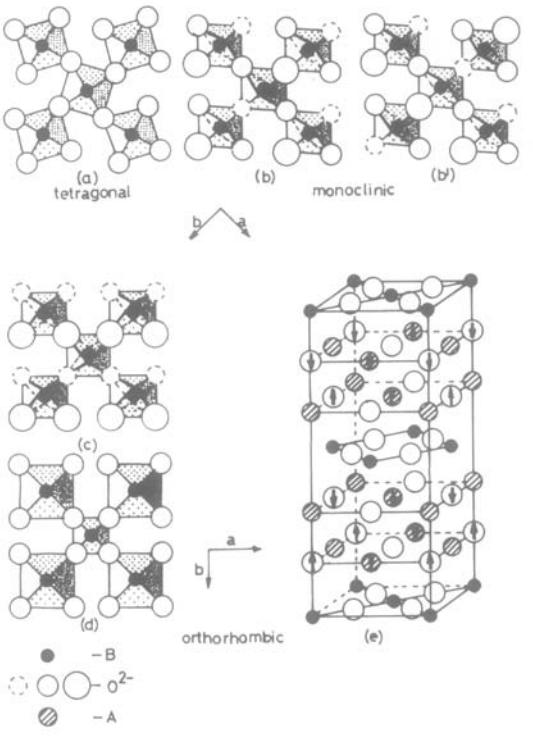

FIG. 5. (a) Rotation of BO_6 octahedra along the c axis; (b, b') Tilting of the octahedra in the ⟨100⟩ direction by rotation along the b axis, the sense of rotation for adjacent B ions along the b axis being different in (b), and the same in (b'); (c) Tilting of octahedra in the ⟨110⟩ direction. Larger circles are above the plane of the paper and broken circles are below the plane. (d) BO_6 octahedra with different B–O_{II} and possibly B–O_I distances (e) Movement of A–O_I–A linkages (Ref. (*13*)) to give rise to O or O' structures.

Sm_2CoO_4 which has the $Fmm2$ symmetry with two Sm–O_I and Co–O_I distances (*8*); the BO_6 octahedra in this oxide may be arranged as in Fig. 5d. Although the orthorhombic nature of the unit cell is apparent in Fig. 5c (with the a' parameter greater than the b' parameter), the orthorhombic nature of the distortion in the O structure is not apparent from Fig. 5d. The O structure has been considered (*13*) to be due to a change in the A–O_{Ib}–A angle from 180° along the b direction by a shift of the A–O_{Ia}–A linkages along the a direction as shown in Fig. 5e ($a > b$).

In a study of the evolution of the tetragonal (T) K_2NiF_4 structure as a function of x in the series $La_{1-x}Y_xCaCrO_4$ and as a function of temperature in $CaYCrO_4$, it has been found that the sequence $O' \rightarrow O \rightarrow T$ occurs in both cases (*13*). Furthermore, as the O phase approaches the O' phase, the b parameter decreases, but the a parameter remains constant. This is consistent with a continuous decrease in the A–O_{Ib}–A angle. In the O' phase, decreasing t or temperature, has the opposite effect (b remaining nearly constant and a decreasing rapidly). This can be understood by assuming that in the O' phase, the A–O_{Ib}–A angle resists further reduction and that the decrease in the tolerance factor imposes a strain on the A–O_{Ia}–A linkage (*15*). Since the A–O_{Ia}–A angle deviates from 180° in this phase, a approaches b with decreasing t. Accompanying these changes the B–O_{II}–B angle also changes in the O' phase and the BO_6 octahedra get tilted as shown in Fig. 5c. It would thus appear as though the O structure is superimposed on the O' structure shown in Fig. 5c so that one may expect two different B–O_I distances even in the O' phase (*15*). This has, however, not been observed in the crystal structures of La_2CoO_4 or La_2CuO_4 (*8, 14*).

The truly monoclinic (M) distortion with $a \neq b \neq c$ and $\gamma \neq 90°$ has not been reported so far. Pr_2NiO_4 and Nd_2NiO_4 were reported to be monoclinic (*9*), but with $a = b$, so that the unit cell can be indexed on the basis of an orthorhombic cell. On rechecking the lattice parameters of Pr_2NiO_4 (*15*), it is found that the structure is indeed truly monoclinic with $a \neq b$. We have observed that $La_2NiO_{4+\delta}$ on heating for long periods in CO_2 at 1150°C gives rise to a monoclinic structure with $a \neq b$; in such a sample, δ would be zero or even slightly negative. As mentioned earlier, small amounts of Ni^{3+} seems to stabilize the tetragonal structure of La_2NiO_4.

The tetragonal to monoclinic distortion

could be associated with changes in the tolerance factor. The monoclinic structure would be associated with the tilting of the BO_6 octahedra of the type shown in Fig. 5b; the sense of tilting of the octahedra between nearest neighbor B ions may be assumed to be the same for a row of octahedra along the b or a axes (Fig. 5b′).

Another modification of the tetragonal K_2NiF_4 structure is the tetragonal T' structure (Fig. 6) found in the copper oxides (*17, 18*) Ln_2CuO_4 (Ln = Pr, Nd, Sm, Eu, Gd). The small c/a ratio of the Ln_2CuO_4 compounds was initially associated with compressed CuO_6 octahedra (*7*) in the same manner as compressed CuF_6 octahedra were initially postulated in K_2CuF_4 (*19*). In the oxides, the a parameter is ~3.97 Å and in order to obtain compressed octahedra, the Cu–O_I distance should be less than 1.98 Å. The suggestion of Longo and Raccah (*7*) that CuO_6 octahedra are compressed is therefore subject to some doubt. The T' structure is derived form the T structure by a shift of the oxide ions from the (*0, 0, z*) positions in the T structure to (0.5, 0.0, 0.25) position in the T' structure. As a consequence, the oxide ion changes its coordination from 6 to 4 in the T' structure. In such a structure, the rare earth and Cu ions have no intervening anion along the c axis. The structure appears to be specific to Cu^{2+} ions (*15*) as the $d^2_{z^2}$ electrons can provide sufficient screening to minimize repulsion between the Cu^{2+} and Ln^{3+} ions. The relationship between K_2NiF_4 related structures and the T' structure has been examined by Singh *et al.* (*20*) in the case of the solid solutions, $La_{2-x}Ln_xCuO_4$ (Ln = Pr, Nd). A first-order transition occurs between the two structures as a function of x accompanied by a marked increase in the volume of the unit cell of the T' phase across the critical value x_c; x_c decreases with the decreasing size of the Ln^{3+} ion. The T' structure may be considered to be composed of alternating layers of $(CuO_2)^{2-}$ layers with the Cu^{2+} ions in the square-planar, fourfold coordination and $(Ln_2O_2)^{2+}$ layers with the fluorite structure containing Ln^{3+} ions in the eightfold coordination. The increase in volume in the T' phase is attributed to the lower packing efficiency while the collapse in the c/a ratio is attributed to the change from the rock-salt-like packing of the $(Ln_2O_2)^{2+}$ layers in the K_2NiF_4 structure to the fluorite type of packing in the T' structure.

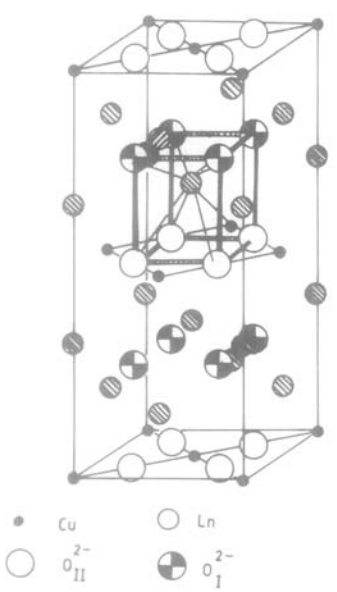

FIG. 6. The T' structure of Ln_2CuO_4 compounds.

The driving force for the transition from the K_2NiF_4 related structure to the T' structure in the $La_{2-x}Ln_xCuO_4$ compounds can perhaps be understood in terms of the competition between the A and B ions for covalency with the O_I ion in the A–O_I–B linkages. The higher acidity of the smaller Ln^{3+} ion could further elongate the Cu–O_I bond (compared to that in La_2CuO_4) and drive the Cu^{2+} ions to a square-planar coordination.

It is interesting that the relationship between Ln_2NiO_4 and Ln_2CuO_4 (Ln = Pr, Nd) with respect to the unit-cell volume and c/a ratio is similar to that between K_2NiF_4 and

K_2CuF_4. This would suggest an antiferrodistortive ordering (Fig. 7a) of CuO_6 octahedra enhancing the a parameter to be the driving force for the transition to the T' structure in Ln_2CuO_4 compounds. An antiferrodistortive type of ordering of elongated BO_6 octahedra of the type found in K_2CuF_4 (*21, 22*) would be unstable in A_2BO_4 oxides. In the fluorides of K_2NiF_4 structures ($t \geq 1$), a mechanism which enhances the a parameter would be favored. In A_2BO_4 oxides, since $t < 1$, mechanisms that reduce the a parameter should be operative and it is perhaps for this reason that La_2CuO_4 has a c/a ratio suggestive of ferrodistortive ordering (*18, 22*) of elongated CuO_6 octahedra (Fig. 7b).

The relationship between the O (or O'), T, M, and T' structures may be obtained from a study of the solid solutions of La_2NiO_4 (T) and La_2CuO_4 (O) and that between Pr_2NiO_4 (M) and Pr_2CuO_4 (T'). In the series $La_2Ni_{1-x}Cu_xO_4$, the O structure

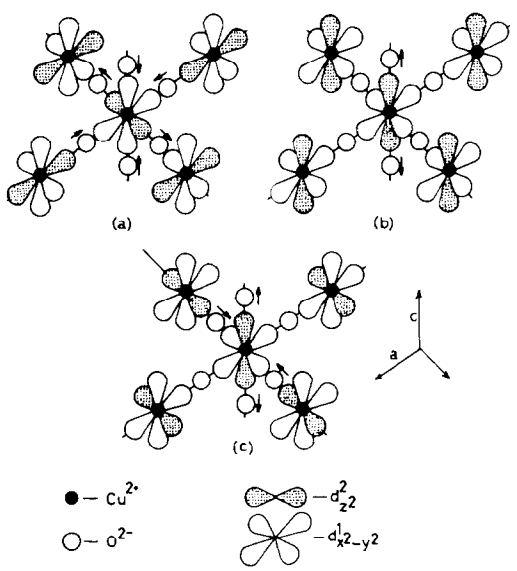

FIG. 7. (a) Antiferrodistortive ordering of elongated CuO_6 octahedra (arrows indicate direction of displacement of oxide ions). (b) Ferrodistortive ordering of elongated CuO_6 octahedra. (c) Ordering of elongated CuO_6 octahedra as in the ac or the bc planes of $KCuF_3$.

is obtained (*20*) from the T structure for $x \geq 0.9$. Since $\beta_{Cu} > \beta_{Ni}$, the changes may be considered to be due to changes in the tolerance factor. However, in the $Pr_2Ni_{1-x}Cu_xO_4$ series (*15*), the M structure which is stable in the range $0 < x \leq 0.1$ goes over to the T structure for $0.25 \leq x \leq 0.50$. In the range $0.50 < x < 0.90$, a mixture of T and T' phases is obtained. For $0.9 \leq x \leq 1.0$, the T' structure is obtained. The $M \rightarrow T$ transition in $Pr_2Ni_{1-x}Cu_xO_4$ is in the opposite direction to that expected from tolerance factor effects. Both the O and O' structures are found (*13*) in oxides of the formula $La_{1-x}Y_xCaCrO_4$ which have high tolerance factors. The fact that such a distortion has not been observed (*23*) in $CaYAlO_4$ probably implies that distortions in $La_{1-x}Y_xCaCrO_4$ are associated with the high energy required to distort the CrO_6 octahedra so that the $Ca-O_{Ic}$ and $Y-O_{Ic}$ distances are constrained to be different. This is in effect reduces the tolerance factor just as Jahn–Teller effects associated with Cu^{2+} ions could enhance it. The immiscibility range in the $Pr_2Ni_{1-x}Cu_xO_4$ solid solutions is consistent with the requirement that two d_{z^2} electrons are necessary to be stabilize the T' structure.

2.2. Ratios c/a and the nature of A–O and B–O bonds in A_2BO_4 oxides. When the tolerance factor $t = 1$, there is a perfect match of the B–O–B and A–O–A distances, in both perovskites and A_2BO_4 oxides. When $t < 1$, the situation in A_2BO_4 oxides is different from that in perovskites. In the latter, there is buckling of the three-dimensional corner-shared octahedral network tending to make the B–O–B angle less than 180° so that the effective B–O–B distance is reduced. In A_2BO_4 oxides, however, the intervening rock-salt layer imparts a rigidity to the two-dimensional octahedral network and prevents the buckling of the octahedra. Instead, there is a pressure effect on the B–O_{II}–B bond tending to reduce the distance while the A–O_I–A distance is stretched in

order that the two distances match in the tetragonal K_2NiF_4 structure. In most oxides including Sr_2TiO_4, $t < 1$ and hence the B–O_{II}–B distance would be expected to be smaller than that computed from the ionic radii. As a consequence, we would expect the B–O_I bond to be lengthened and the A–O_I bond to be shortened. Accordingly, fluoride ions in Sr_2FeO_3F substitutes for the O_I ions in keeping with the weaker B–O_I bond strength (*24*).

Evidence for covalent Ln–O_I bonding in $LnSrBO_4$ and Ln_2BO_4 compounds may also be obtained indirectly by the application of the method of invariants. Poix (*3*) has applied successfully the method of invariants (Eq. (3)) to oxides of the formula Sr_2BO_4 and to other oxides where the B ions are in the 4+ state. We have evaluated the value of ψ_{Ln} for a series of compounds of the type Ln_2BO_4 and $LnSrBO_4$ (Table I) and find that ψ_{Ln} is not really an invariant. The reason for this may lie in the covalency of the Ln–O_I bonds and the possible competition between Ln–O_I and B–O_I bonds.

Elongation of the BO_6 octahedra in A_2BO_4 type oxides can lead to the stabilization of unusual electronic configurations of the B ions. Thus, intermediate-spin Co^{3+} ions ($t_{2g}^5 d_{z^2}^1 d_{x^2-y^2}^0$) are found to exist at low temperatures in La_4LiCoO_8 and $LaSrCoO_4$ (*25–27*). At high temperatures, they are transformed to the high-spin configuration ($t_{2g}^4 e_g^2$). High-spin Fe^{4+} ions are found in $La_3SrLiFeO_8$ (*28*). In La_4LiNiO_8, ESR and magnetic susceptibility studies (*29*) have shown that the Ni^{3+} ions are in the low-spin ($t_{2g}^6 d_{z^2}^1 d_{x^2-y^2}^0$) configuration. In Sr_2FeO_3F, the Fe^{3+} ions are in the low-spin configuration due to the apical positioning of the fluorines (*24*); Sr_4FeTaO_8 also seems to show Fe^{3+} ions in the low-spin configuration (*16*).

Elongated BO_6 octahedra, short B–O_{II}–B bonds as well as short A–O_{Ic} bonds (A–O_I bonds along the c axis), are commonly found in many of the A_2BO_4 oxides. Thus, in $LaSrFeO_4$ and $LaSrCrO_4$, the values of the a parameter (3.86 and 3.84 Å, respectively) are considerably smaller than the pseudo-cubic unit cell parameters of $LaFeO_3$ and $LaCrO_3$ (3.931 and 3.883 Å, respectively); similarly, the a parameter of Sr_2TiO_4 (3.88 Å) is smaller than that of $SrTiO_3$ (3.90 Å). In general, pressure on the B–O_{II}–B distance increases as t decreases from unity or as the size of the B ion increases (or the formal charge decreases). Accordingly, the B–O_{II} distance in La_2NiO_4 is 1.93 Å (*6*) compared to the value of 2.09 Å in NiO (*30*). The A–O_{Ic} distance would be expected to decrease as the charge of the A ion increases. In La_2NiO_4, the La–O_{Ic} distance (*2, 11*) is around 2.36 Å compared to the value of 2.616 Å computed from ionic radii (*16*).

Pressure effect on the B–O_{II}–B bond can be viewed in another manner. Along the c axis, there are A–O_I–B–O_I–A $\cdots$ A–O_I–B–O_I–A linkages. There would be strong electrostatic repulsion between $A \cdots A$ ions with no intervening anions between them. The O_{II} ions in the basal plane could come closer and screen the charge of the A ion and thereby reduce the a parameter. Electrostatic repulsion between the A ions could push the A ions closer toward the O_{Ic} ions. Strong A–O_I bonding would reduce the effective charge on the A ion and hence the $A \cdots A$ electrostatic repulsion. If we consider the ionic potential of A ions, we would expect the smaller ions to increase the $A \cdots A$ electrostatic repulsion. Furthermore, because of the competition between A and B ions for bonding with O_I ions, the A–O_{Ic} bond will get shorter (and the B–O_I bond longer or BO_6 octahedra elongated) as the charge on the A ion increases. Accordingly La–O_{Ic} bond distances in $LaSrAlO_4$ and La_2NiO_4 are 2.53 and 2.40 Å, respectively (*6, 15*). A compression of the BO_6 octahedra may therefore be taken to indicate a weakening of the A–O_{Ic} interaction.

It is interesting to examine the variation of the lattice parameters and the c/a ratios

in $LnSrBO_4$ (Ln = rare earth) type compounds with the size of the rare earth ion. In general, the a parameter shows a linear dependence on the size of the rare earth ion. In Fig. 8, we have shown the variation of the c/a ratios in a series of compounds of the formula $LnSrBO_4$ (B = Al, Cr, Fe, Ni) with the size of the rare earth ion. In $LnSrAlO_4$ (*15, 31*), there is a linear variation of the a parameter with the size of the Ln ion and a small change in the c/a ratio between Pr and Nd (Fig. 8a). Refinement of the positional parameters has shown (*15*) that the Al–O_I distance in $LaSrAlO_4$ (2.01 Å) is larger than that in $GdSrAlO_4$ (1.95 Å); the Al–O distance computed from ionic radii (*16, 32*) is 1.935 Å. A compression of the AlO_6 octahedra implies that the Gd–O_{Ic} interaction is weaker than the La–O_{Ic} interaction. The average Al–O distance in $LaSrAlO_4$ is 1.92 Å while that in $GdSrAlO_4$ is 1.885 Å. The average (Ln,Sr)–O_{Ic} distance is 2.53 Å in $LaSrAlO_4$ and 2.48 Å in $GdSrAlO_4$ compared to the computed values of 2.66 and 2.61 Å for the (La,Sr)–O and (Gd,Sr)–O distances and 2.62 and 2.51 Å for the La–O and Gd–O distances. While the Gd–O_{Ic} distance in $GdSrAlO_4$ is close to that predicted by ionic radii, the La–O_{Ic} distance in $LaSrAlO_4$ is considerably smaller. This would again imply that La–O_{Ic} interaction is stronger than the Gd–O_{Ic} interaction.

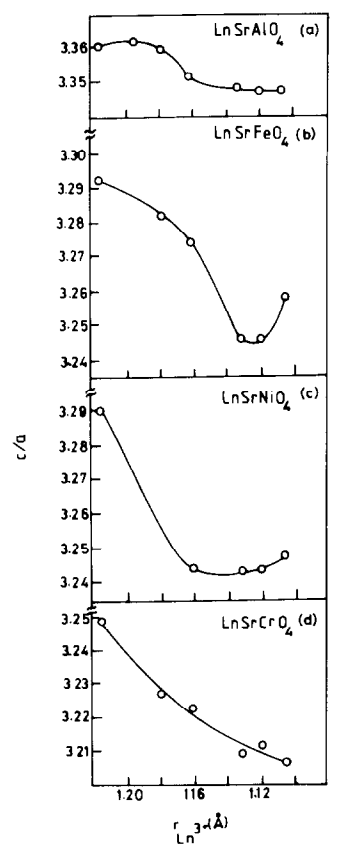

FIG. 8. Variation of the c/a ratio in $LnSrBO_4$ as function of the radius of the Ln ion.

In $LnSrNiO_4$ (*33*), the a parameter decreases linearly with the size of the Ln ion, but there is an abrupt change in the c parameter and in the c/a ratio (Fig. 8c). Since the size of low-spin Ni^{3+} is comparable to that of Al^{3+}, the markedly different behavior of $LnSrNiO_4$ compounds cannot be due to ionic size effects; electronic factors seem to be important. A similar behavior is observed in $LnSrFeO_4$ and $LnSrCrO_4$ (*34*) as can be seen from Fig. 8.

When the A ion is kept constant and the B ion is varied, systematics in lattice parameters are not obvious. In Fig. 9, the lattice parameters and c/a ratios (*35, 36*) of some Sr_2BO_4 compounds are plotted against the ionic radius of the B ion. The a parameter varies linearly with the radius of the B ion provided that it has partially filled d orbitals. Thus, ions such as Sn^{4+}, Hf^{4+}, and Zr^{4+} do not fall on this straight line. Poix (*3*) has, however, found a linear relationship using the β_B parameters. What is important is that there is no linear relationship between the c parameters or the c/a ratios and the size of the B ion in these compounds. Furthermore, compounds containing B ions with partially filled d orbitals exhibit larger c/a ratios than those with filled or empty d orbitals. When the B ions have partially filled d orbitals, the c/a ratio

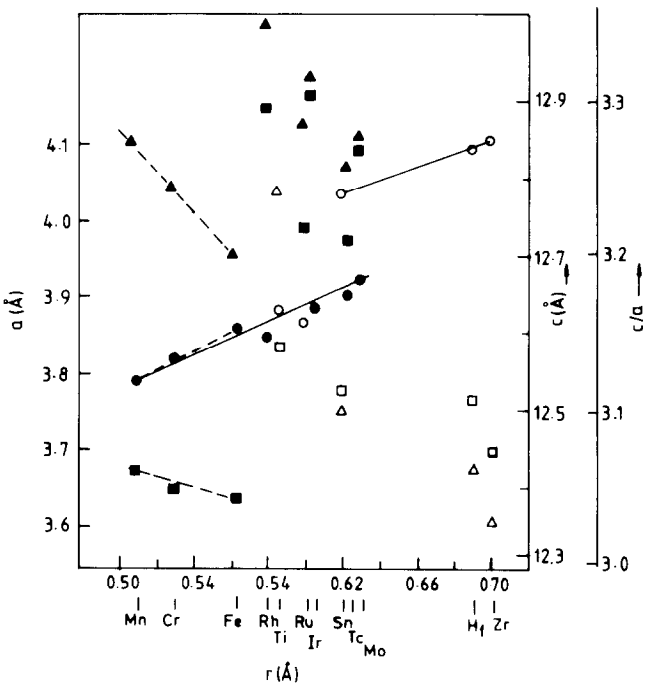

FIG. 9. Variation of the a and c parameters and the c/a ratio of several Sr_2BO_4 compounds with the radius of the B ion: circles, a parameter; squares, c parameter; triangles, c/a ratio; closed symbols represent partly filled d orbitals.

seems to increase with the decreasing size of the B ion (of the same period). In the case of $LaSrBO_4$ compounds (*35*, *36*) even the a parameter does not show systematic changes with the radius of the B ion. In Sr_2BO_4 compounds, the high charge of the B^{4+} ion compared to that of Sr^{2+} ensures that the BO_6 octahedra are regular since the B–O_1 bonds would be much stronger than the Sr–O_{1c} bonds. In $LaSrBO_4$ compounds, however, competition between La and B ions for covalent bonding with the oxygen ions could complicate the situation. When the B ion is a $3d$ transition metal ion such as Mn^{3+} or low-spin Ni^{3+}, further complications enter because of the possibility of static Jahn–Teller distortions.

In Fig. 10, we have plotted the c/a ratios in some $LaSrBO_4$ compounds where the B ion (Fe, Cr, V) is neither a Jahn–Teller ion nor expected to occur in the low-spin state, against the octahedral crystal field stabilization energy (*37*) and the optical electronegativity of the B ion in B_2O_3 compounds (*38*). The linear relationships found here indicate that B ions which do not form strong cova-

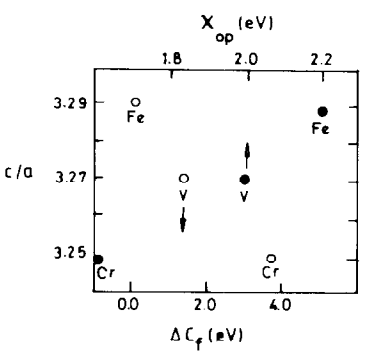

FIG. 10. Variation of the c/a ratio of $LaSrBO_4$ (B = Cr, V, Fe) with the octahedral crystal field stabilization energy, ΔC_f, and the optical electronegativity of the B ions in B_2O_3 compounds.

lent bonds (or which favor an octahedral environment) also favor a low c/a ratio. Thus, we may conclude that when $t < 1$, increasing covalency of the B–O_{II} bond favors an elongation of the BO_6 octahedra. This elongation is a consequence of the pressure on the B–O_{II} bond in the ab plane. In Sr_2BO_4 compounds, $t \approx 1$ and the pressure on the B–O_{II} bond is considerably reduced. Nevertheless, the above considerations account for the high c/a ratios in Sr_2BO_4 compounds containing B ions with partially filled d orbitals. Elongation of the BO_6 octahedra associated with B ions which are Jahn–Teller ions, may favor a cooperative, ferrodistortive ordering of octahedra elongated parallel to the c axis. The unusually high c/a ratios ($\approx$3.40) in La_2CuO_4 and $LaSrMnO_4$ (*7*, *39*) could be indicative of such ordering.

Another feature of A_2BO_4 oxides with the K_2NiF_4 structure is that the average B–O distance is less than that computed from ionic radii especially when t is considerably less than unity. Thus, in La_2NiO_4 and La_2CuO_4, the average Ni–O and Cu–O distances are 2.03 and 2.07 Å, respectively (*6*, *7*), while the values from ionic radii are 2.09 and 2.13 Å, respectively (*16*, *32*). When the average B–O distance is very small, the question arises as to whether a disproportion of B ions can occur. Thus, Cu^{2+} can disproportionate to Cu^{1+} and Cu^{3+}. The average (Cu^{1+}, Cu^{3+})–O distance is coincidentally 2.07 Å, which is the average Cu–O distance in La_2CuO_4 (*7*). Significantly again, the lattice parameters of La_2CuO_4 are close to that of $La_4Li^{+}Cu^{3+}O_8$ (*40*) and the radius of the Li^{+} ion (0.76 Å) is only slightly smaller than that of Cu^{2+} ion (0.77 Å). Although we do not propose that there is actually a static disproportionation of Cu^{2+} ions in La_2CuO_4, the above arguments suggest the possible presence of charge-density waves. Transition metal ions with incompletely filled d orbitals have a mechanism to adjust their ionic radii toward a more favorable value of t by disproportionation or by forming charge-density waves. For example, disproportionation of Fe^{4+} ions into Fe^{3+} and Fe^{5+} ions is known to occur in $CaFeO_3$ (*41*) but not in $SrFeO_3$ with a higher tolerance factor. Studies on Ca_2FeO_4 and Sr_2FeO_4 would be interesting to establish whether the disproportionation is associated with the tolerance factor.

It is clear from the above discussion that the c/a ratio in A_2BO_4 oxides is determined by several factors. Besides the covalency of the B–O_{II}-B bond and the competition between A–O_I and B–O_I linkages, other factors may also be important. Thus, $LaSrCuO_4$ in which the Cu^{3+} ion is in the low-spin state has an unusually high c/a ratio (*40*); the preference for square-planar coordination of low-spin Cu^{3+} ion is possibly an important factor here. $LaNaTiO_4$ and compounds of the formula La_4LiBO_8 (B = Co, Cu, Ni) also have unusually high c/a ratios (*35*, *36*). In the former, the Ti–O–Ti distance is unusually short (3.77 Å) compared to 3.88 Å in Sr_2TiO_4; in line with our earlier arguments, we expect the TiO_6 octahedra to be elongated. Since the LiO_6 octahedra would be elongated because of the short Li-O_{II} distances we would expect increased c/a ratios in La_4LiBO_8 compounds.

2.3. One-dimensional antiferromagnet model of K_2NiF_4 structure. It is instructive to visualize the K_2NiF_4 structure as having a stacking sequence . . . *RPRPRPRPRPRP* . . . where R is a rock-salt layer and P is a perovskite layer. In so doing, we ignore the displacement of alternate perovskite layers mentioned earlier. Such a sequence is formally analogous to a one-dimensional antiferromagnetic Ising chain where R and P are treated as pseudo-spins with anisotropy. Long-range order is provided by an ordering field which can, in principle, arise from several mechanisms.

When t is less than unity, compression of the B–O_{II}–B bond (and expansion of the A–O_I–A bond) is necessitated. Long-range

one-dimensional *RPRPRP* order would be favored because of the higher energy associated with interactions such as *RR* or *PP*.

In compounds with the Ruddlesdon–Popper structures (*42*) such as (SrO) $(SrTiO_3)_n$, compounds with $n = 1$ have an a parameter of 3.88 Å (compared to 3.906 Å in $SrTiO_3$) while the a parameter of compounds with $n = 2$ and 3 is 3.90 Å, implying that in these compounds, the perovskite layer cannot be compressed. Furthermore, since the Ti–O–Ti distance in these oxides is larger than the $(1/\sqrt{2})$ A–O–A distance, it would require considerable energy to stretch the Sr–O bond in a bilayer of SrO. Consequently, compounds of the type $(SrO)_m$ $(SrTiO_3)_n$ are not known including the type $m = n = 2$ shown in Fig. 3e. The $(AX)_m$ $(ABX_3)_n$ system may be possible, however, with larger A ions and it would be interesting to investigate systems such as $LaMBO_4$ (M = monovalent ion) and Ba_2TiO_4–Sr_2TiO_4 where Ba_2TiO_4 has the K_2SO_4 structure with Ti in the tetrahedral site (*43*). In compounds such as La_2BO_4, the $(LaO)^+$ layer is positively charged while the $(LaBO_3)^-$ layer is negatively charged. The stacking sequence in such oxides is therefore a favorable one for ordering along the c axis, . . . R^+ P^- R^+ P^- R^- P^- R^+ . . . In oxygen excess $La_2BO_{4+\delta}$ compounds (e.g., La_2NiO_4), if the δB^{3+} ions are randomly distributed, the $LaBO_3$ layers would be electricaly neutral (P^0). We can then have intergrowths of P^- P^0 and P^- P^0 P^0 type of layers; intergrowths of the composition $La_3Ni_2O_7$ and $La_4Ni_3O_{10}$ have been observed (*44*) in oxygen-excess La_2NiO_4. Tilley (*45*) has carried out an electron microscopic investigation of the SrO–TiO_2 system with special reference to Sr_2TiO_4. Besides the intergrowth of Ruddlesdon–Popper phases such as $Sr_3Ti_2O_7$ and $Sr_4Ti_3O_{10}$, intergrowth of SrO-rich phases has been observed by Tilley. In the La_2BO_4 phases, intergrowth of two $(LaO)^+$ layers adjacent to each other would not be likely unless at least one of the LaO layers adjusts its oxygen and La content in such a manner as to make the layer neutral. Since this is unlikely, some La_2O_3 should be precipitated out in oxygen-excess La_2BO_4 compounds. Another possibility is that the excess oxygen is accommodated by A-site deficiency. In compounds such as Sr_2BO_4, R and P layers are both neutral and intergrowth of *RR* and *PP* sequence would be possible.

2.4. Superlattice ordering in A_2BO_4 compounds. Ordering of B ions in compounds of the type $A_2BB'O_4$ due to charge difference potential between B and B' ions in different oxidation states would be analogous to antiferromagnetic ordering of spins in K_2NiF_4 due to an exchange potential. Since a three-dimensionally ordered antiferromagnetic structure of K_2NiF_4 is known (*1*), it seems reasonable to expect that B and B' ions may similarly get ordered. However, not all possible antiferromagnetic interactions can be satisfied in the K_2NiF_4 structure (*46*) and this frustration leads to a two-dimensional order.

In compounds such as La_4LiBO_8 (B = Co, Ni, or Cu) or $Sr_4BB'O_8$ (B = Co, Fe, Ni, etc.; B' = Nb, Ta), X-ray diffraction studies do not reveal any evidence for an ordered superlattice (*47, 48*). Demazeau *et al.* (*25*) have found evidence for a $\sqrt{2}$ increase in the tetragonal a parameter by employing neutron diffraction and X-ray diffraction (with monochromatized Cu $K_{\alpha 1}$ radiation) in La_2LiCoO_8. Our electron diffraction studies also reveal such ordering as mentioned earlier; the electron diffraction patterns of La_4LiCoO_8 show streaking parallel to the c^* axis (Fig. 4c) similar to the ridges found in the neutron diffraction pattern of K_2NiF_4 in the temperature range where there is only two-dimensional antiferromagnetic ordering (*1*). We feel that the streaking in Fig. 4c may indeed be associated with two-dimensional ordering of Li^+ and Co^{3+} ions.

Three-dimensional antiferromagnetic ordering in K_2NiF_4 is associated with an orthorhombic distortion. It is interesting that the distortion which gives rise to *M*, *O*, and *O'* structures involves the movement of O_I ions along the *c* axis (Fig. 4) besides that of O_{II} ions in the *ab* plane. By analogy with the three-dimensional antiferromagnetic ordering in K_2NiF_4, we would expect three-dimensional ordering of *B* ions in A_2BO_4 only in distorted structures or when *t* is close to 0.85.

In A_2BO_4 oxides, there are eight *A* ions surrounding the *B* ions as in the perovskite structure and two *A* ions linked through O_I ions with the *B* ions along the *c* axis. Random occupation of these sites by La and Sr ions in $LaSrBO_4$ (*33*) could give rise to a distribution of crystal fields. Of these, the most important are those involving the O_I ions. La–O_I–B–O_I–La arrangement would give rise to the lowest crystal field while Sr–O–*B*–O–Sr arrangement would give rise to the highest crystal field. Evidence for a distribution of sites is seen in the Fe^{3+} ESR spectra of $LaSrAl_{0.98}Fe_{0.02}O_4$ (Fig. 11). There are two prominent lines at $g \approx 6$ and $g \approx 4.25$ which may be associated with Fe^{3+} ions in axial and orthorhombic symmetry (*49–51*); the $g \approx 6$ line is also found in oxide glasses containing Fe^{3+} (*51*). There is also a line at $g \approx 2.1$. The deviation from $g = 2$ may be attributed to spin-orbit coupling effects in Fe^{3+} ions in distorted octahedra. Similarly, $LaSrAlO_4$ containing small amounts of Ni^{3+} ions clearly shows evidence for the simultaneous existence of low-spin and high-spin Ni^{3+} ions (*52*). Random ordering of *B* ions in LaSr $(B,B')O_4$ has been used to explain percolation effects in electrical and magnetic properties of these compounds (*16*, *52*).

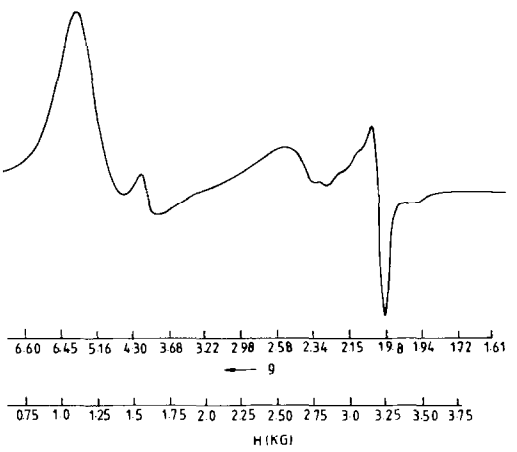

FIG. 11. ESR signal from Fe^{3+} ions in $LaSrAl_{0.98}Fe_{0.02}O_4$.

The only $AA'BO_4$ compound which shows ordering is $LaNaTiO_4$ (*53*). Ordering in this compound interestingly involves $(La_2O_2)^{2+}$ and $(Na_2O_2)^{2-}$ layers (*53*). There is considerable pressure on the Ti–O_{II}–Ti bonds in $LnNaTiO_4$ ($a \approx 3.78$ Å compared to 3.88 Å for Sr_2TiO_4), consistent with the low tolerance factor. As discussed earlier, a structure containing bilayers of rock-salt and perovskite (Fig. 3e) such as $(Ln_{0.5}Na_{0.5}O)_2$ $(Ln_{0.5}Na_{0.5}TiO_3)_2$ would also impose considerable pressure on the Ti–O_{II}–Ti bond. We have observed that X-ray diffraction line intensities calculated for such a structure by assuming a random distribution of *Ln* and Na ions are comparable to those reported by Blasse (*53*).

2.5. Non-stoichiometry. Oxides with the K_2NiF_4 structure can accommodate considerable non-stoichiometry. This could lead to a significant variation in lattice parameters as indeed found in oxides such as LaSr FeO_4, Pr_2NiO_4, or Nd_2NiO_4, (*9*, *10*, *15*, *54*). In the $La_2NiO_{4+\delta}$ system, Drennan *et al.* (*44*) have shown that intergrowth of Ruddlesdon–Popper type phases such as $La_3Ni_2O_7$ and $La_4Ni_3O_{10}$ would account for anion-excess non-stoichiometry. Lewandowski *et al.* (*55*) have found *A*-site deficiency in lanthanum cobalt oxide; such a defect structure would be favored by δB^{3+} ions.

Oxygen-deficient non-stoichiometry is more difficult to account for. Poeppelmeier

et al. (*56*) have observed that $Ca_2MnO_{3.5}$ can be obtained topotactically from Ca_2MnO_4 by reduction, just as $CaMnO_{2.5}$ can be obtained from $CaMnO_3$. In $CaMnO_{2.5}$, Mn^{3+} ions are in five-coordinated square-pyramidal coordination. It is assumed that the same situation may be present in $Ca_2MnO_{3.5}$. The idealized structure proposed for $Ca_2MnO_{3.5}$ is shown in Fig. 12 with the O_{II} atoms being labile. The loss of O_{II} atoms instead of O_I atoms is consistent with $t < 1$; since the B–□–B (□ = vacancy) distance would be smaller than the B—O_{II}—B distance, it would favor the K_2NiF_4 structure. In Sr_2CuO_3, half the O_{II} oxygen sites are vacant (*18*) and this is possible with Cu^{2+} because of the presence of $d^2_{z^2}$ electrons. In this laboratory, a layered brownmillerite phase of the formula $Ca_2FeO_{3.5}$ (a = 14.768, b = 13.724, and c = 12.20 Å) has been recently synthesized (*57*). This structure seems to have alternate columns of octahedra and tetrahedra in the ab plane with oxygen vacancies in both O_I and O_{II} positions. It is possible that in $Ca_2MnO_{3.5}$, fivefold coordination of Mn is achieved by the loss of O_I oxygens. In any case, it is important to to note that anion-deficient non-stoichiometry can be achieved by the loss of O_I or O_{II} oxygens.

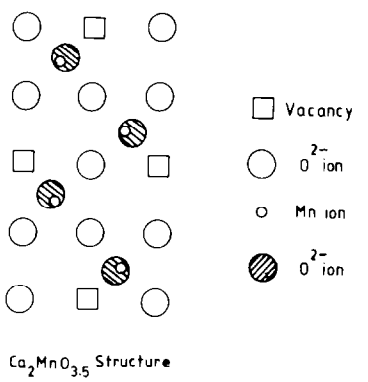

FIG. 12. Proposed ordering scheme in the ab plane of fivefold coordinated Mn^{3+} ions in $Ca_2MnO_{3.5}$. Oxide ions above the plane of the paper and Ca ions are not shown (from Ref. (*56*)).

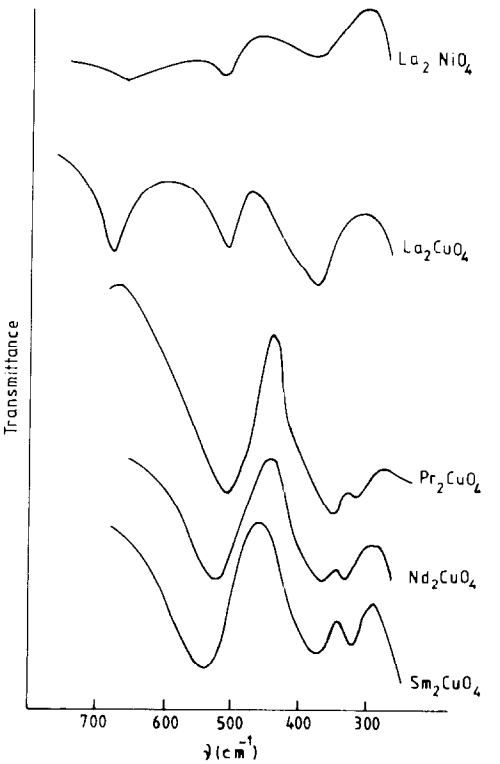

FIG. 13. Infrared spectra of some Ln_2BO_4 compounds.

3. Infrared Spectra

Infrared spectra of A_2BO_4 type oxides provide useful, diagnostic information on the nature of the BO_n polyhedra. Thus, the spectra clearly distinguish Ln_2CuO_4 compounds of orthorhombic structure containing distorted CuO_6 octahedra from those of tetragonal structure containing square-planar CuO_4 polyhedra. We see from Fig. 13 that the Cu–O asymmetric stretching vibration band is split into a doublet (~690 and 520 cm^{-1}) in La_2CuO_4 (suggesting D_{4h} symmetry of the isolated octahedron), while it appears as a single band in other Ln_2CuO_4 compounds with square-planar coordination. The spectrum of La_2NiO_4 possessing distorted NiO_6 octahedra is similar to that of La_2CuO_4. In the spectra of $La_{2-x}Pr_xCuO_4$, Cu–O asymmetric stretching is a

doublet when $x < 0.75$ and a single band when $x \geq 0.75$ and Cu coordination is square-planar. In $LaSrBO_4$ (B = Al or Fe), there seem to be three bands in the B–O stretching region suggesting a low symmetry of the BO_6 octahedra. The B–O stretching mode in $LaSrBO_4$ shifts to higher frequencies compared to that in the corresponding La_2BO_4. It is interesting that the B–O stretching frequency in $AA'BO_4$ oxides is higher compared to that in the corresponding ABO_3 perovskites. In $GdSrAlO_4$, for instance, the $Al–O_{II}$ stretching frequency increases by as much as 75 cm^{-1} compared to that in $GdAlO_3$ and by about 50 cm^{-1} compared to that in $LaSrAlO_4$. The Al–O stretching frequencies in $LaAlO_3$ and $GdAlO_3$ are similar, consistent with our earlier observation that in ABO_3 perovskites, lowering of t leads to a buckling of the octahedra, the B–O distance remaining roughly the same. In A_2BO_4 oxides, the layered structure does not allow buckling and there is greater pressure on the $B–O_{II}–B$ bond with decreasing t.

4. Magnetic Properties

4.1. Spin-state equilibria of transition metal ions. Transitions between low-spin and high-spin states of transition metal ions have been found in perovskite oxides (*58, 59*) such as $LaCoO_3$. There is evidence for such transitions between spin states in oxides of K_2NiF_4 structure as well. The earliest evidence for such a transition was obtained with La_4LiCoO_8 by Blasse (*60*). Because of the elongated nature of the BO_6 octahedra in this oxide, the degeneracy of the e_g orbital is expected to be lifted, shifting the $d_{x^2-y^2}$ orbital to higher energies. This orbital can remain unoccupied under certain conditions and this indeed appears to be the case with Co^{3+} ions in La_4LiCoO_8. In Fig. 14, we have shown the inverse susceptibility–temperature curve of La_4LiCoO_8 and this is best interpreted in terms of a low-spin to intermediate-spin state transition. The intermediate-spin state with the configuration $t_{2g}^5 d_{z^2}^1 d_{x^2-y^2}^0$ seems to be stabilized (at intermediate temperatures) in compounds such as La_4LiCoO_8 (*25*) and also perhaps in Sr_4CoNbO_8 and Sr_4CoTaO_8 (*52*). In the last two compounds, there is some evidence of ordering of the two spin state (just as in $LaCoO_3$), the inverse susceptibility–temperature curve showing a plateau.

An interesting example of spin-state equilibrium between low- and high-spin Ni^{3+} ions has been reported in $LaBaNiO_4$ on the basis of ESR evidence (*61*). The average Ni–O distance of 2.03 Å in this compound is consistent with the Ni–O distance expected from the ionic radius of high-spin Ni^{3+}. Magnetic susceptibility studies (*52*) on $LaSr_{1-x}Ba_xNiO_4$, however, reveal that the susceptibility can be entirely described on the basis of an equation of the form $\chi = [C/(T + \theta)] + \alpha$ where α is of the order of 6×10^{-4} emu and C is of the order of 0.01–0.1 emu/K; C increases with increasing x while θ (in the range 10–20 K) decreases with increasing x. Magnetic susceptibility measurements show no evidence for an activated behavior. It would therefore seem that most of the e_g electrons of the Ni^{3+} ions are in extended states (as in $LaSrNiO_4$,

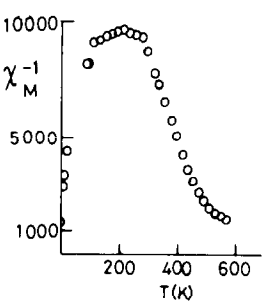

FIG. 14. χ_M^{-1} vs T plot of La_4LiCoO_8 (after Ref. (*25*)).

with $x = 0$, where the $d_{x^2-y^2}$ electrons from a $\sigma^*_{x^2-y^2}$ band) with only a few of the electrons being localized. Localized electrons in $LaBaNiO_4$ may be associated with Ni sites with high crystal field, introduction of Ba^{2+} in $LaSrNiO_4$ increasing the number of localized Ni^{3+} states along with the unit-cell volume. It is possible that the ESR evidence of Demazeau *et al.* (*61*) is associated with such localized states.

An unusual configuration change of low-spin Ni^{3+} has been observed (*52*) in the solid solution $LaSrAl_{1-x}Ni_xO_4$. For small values of x, the Ni^{3+} ions are predominantly in the low-spin state showing an ESR signal similar to that observed in La_4LiNiO_8 (*29*) in which the Ni^{3+} ions have the configuration $t^6_{2g}d^1_{z^2}d^0_{x^2-y^2}$. For $x \geq 0.75$, the ESR signal disappears and the magnetic susceptibility decreases sharply. The change in magnetic properties is accompanied by a significant decrease in the c/a ratio. This points to a change to the configuration t^6_{2g} $d^0_{z^2}d^1_{x^2-y^2}$ with the $d_{x^2-y^2}$ electrons forming $\sigma^*_{x^2-y^2}$ band-like states. It is significant that the magnitude as well as the temperature dependence of the susceptibility of the $x = 0.75$ sample (*52*) is close to that of pure $LaBaNiO_4$. It seems therefore extremely unlikely that the bulk of the Ni^{3+} ions in the latter compound are involved in a low-spin to high-spin transition.

4.2. Antiferromagnetic ordering. When the A ion is nonmagnetic and the B ion is magnetic, A_2BO_4 oxides may be expected to behave as the fluorides with strong intralayer coupling and weak interlayer coupling. The earlier study (*62*) of such an oxide was on Ca_2MnO_4. In this oxide, Mn^{4+} ions are coupled antiferromagnetically with the spins parallel to the c axis. The magnetic structure determined by neutron diffraction (*62*) is shown in Fig. 15. Interplanar magnetic ordering leads to a doubling of the unit-cell parameter. Poeppelmeier *et al.* (*56*) have recently reported that the c parameter of Ca_2MnO_4 is actually twice that of the value reported earlier. Considerable work has been carried out at Bordeaux on magnetic ordering in insulating A_2BO_4 oxides in which the spins couple antiferromagnetically. In Fig. 15, we show the magnetic structure of β-Sr_2MnO_4 (*63*) and $LaCaFeO_4$. In the latter, the magnetic moments are aligned along the a axis.

Le Flem *et al.* (*64*) have pointed out that β-Sr_2MnO_4 (*63*), $LaSrCrO_4$ (*65*), and La-rich $La_{1-x}Y_xCaCrO_4$, show strong two-dimensional behavior as indicated by the critical exponents in the vicinity of the ordering

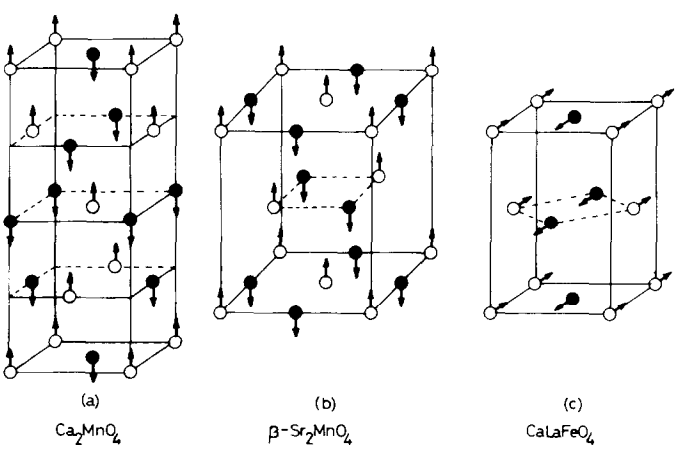

FIG. 15. Magnetically ordered structure of (a) Ca_2MnO_4, (b) β-Sr_2MnO_4, and (c) $LaCaFeO_4$ (from Ref. (*64*)).

temperatures as well as by neutron scattering investigations. Compounds such as Ca_2MnO_4 and $CaYCrO_4$ have essentially three-dimensional magnetic correlations. These authors also point out that the change from two-dimensional to three-dimensional correlation depends on the extent of covalency of the A–O bond. Making use of Goodenough's arguments in the case of perovskites (*66*), these authors suggest that there is competition between t_{2g}–O_{II}–t_{2g} interaction (involving the t_{2g} orbitals of the B ions) and $\sigma_{A-O_{II}}$ bonding (involving the A ions in the perovskite layer with a 90° A–O_{II}–B linkage). The greater the covalency of the A–O_{II} bonding, the weaker is the B–O_{II}–B interaction and the stronger is the three-dimensional coupling. Thus, ions such as Cr^{3+} and the isoelectronic Mn^{4+} with only t_{2g} electrons, have their magnetic interactions strongly determined by the nature of A–O interactions. The smaller the A cation, the stronger is the A–O_{II} linkage (and the three-dimensional correlations) and the lower is the antiferromagnetic ordering temperature. Applying the same arguments to oxides containing Fe^{3+} ions, it is stated that since the magnetic interactions are strongly determined by the e_g electrons, the influence of the A ion is considerably diminished. Accordingly, there is not much difference in the ordering temperatures of $LaCaFeO_4$ (373 K) and $LaSrFeO_4$ (380 K). However, compounds such as LnSrFeO$_4$ show a marked dependence of the magnetic ordering temperature on the size of the Ln ion (*67*). Although the above arguments seem plausible, we should note that we have ignored the A–O_I–B linkage which would be exected to play a role. The collapse in the c/a ratio of LnSrBO$_4$ compounds with the decreasing size of Ln ion (Fig. 4) is consistent with a decreased B–O_I distance. Since the B–O_I–O_I–B interaction determines the interlayer coupling, we may expect the three-dimensional character to increase with decreasing B–O_I bond length.

In $LaSrAl_{1-x}Fe_xO_4$ solid solutions (*15*), the Néel temperature drops to zero when $x > x_c$ where x_c (0.59) is the critical percolation threshold for nearest-neighbor interactions in a square-planar array (*68*). The results are similar to those found in the $Rb_2Mg_{1-x}Mn_xF_4$ system (*69*). The surprising conclusion, therefore, is that even in oxides, long-range magnetic ordering is dominated by nearest-neighbor interactions.

4.3. Unusual Behavior of La_2NiO_4, La_2CuO_4, and La_2CoO_4. La_2NiO_4 shows a Curie–Weiss behavior at high temperatures with high θ (~ −500 K) and μ_{eff} (~3.00 μ_B) values (*70*). Below 200 K, there is deviation from the Curie–Weiss law, but neither neutron diffraction nor magnetic susceptibility studies down to the lowest temperature show any evidence for long-range antiferromagnetic ordering (*70, 71*). It has been found recently that below 100 K, the magnetic susceptibility again conforms to a Curie–Weiss behavior of (Fig. 16) with a μ_{eff} of

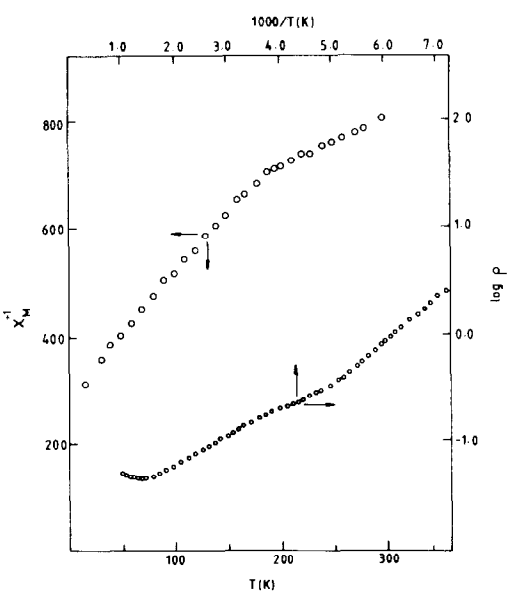

FIG. 16. Plots log ρ vs $1/T$ and χ_M^{-1} vs T of La_2NiO_4 (from Ref. (*2*) and unpublished results from this laboratry).

1.8 μ_B indicating the presence of one unpaired electron (*15*). The θ value obtained from the slope of the χ_M^{-1} vs T plot is consistent with the expression $\theta = CW$ with a nearly temperature-independent W and with a C corresponding to two unpaired electrons above 200 K and one unpaired electron below 100 K. Such a behavior is also observed in the $La_2Ni_{1-x}Cu_xO_4$ system in the range $0.75 \geq x \geq 0.0$ below 100 K with a μ_{eff} value corresponding to one unpaired electron (*15*) per g. atom of Ni. Below 200 K, there is also an increase in the activation energy for electrical conduction (Fig. 16) suggesting that there is spin-pairing of the $d_{x^2-y^2}$ electron around 200 K. It is rather surprising that in La_2NiO_4, below 200 K, the $d_{x^2-y^2}$ electrons are coupled into nearly dimagnetic spin-paired states while the d_{z^2} electrons are localized and coupled antiferromagnetically without the onset of long-range order. Since La_2NiO_4 prepared by ceramic techniques always has an excess of oxygen due to the presence of Ni^{3+} ions, it is not clear whether long-range order is frustrated by the presence of such ions. Singh *et al.* (*15*) propose that a disproportionation of the Ni^{2+} ions to Ni^{1+} and low-spin Ni^{3+} (which could result in the formation of charge-density waves) would stabilize the diamagnetic nature of the spin-paired states involving the $d_{x^2-y^2}$ electrons.

La_2CuO_4 was first reported to show nearly temperature independent magnetic susceptibility which was attributed to antiferromagnetism (*7*). Because of the low value the electrical resistivity, it was assumed that the oxide exhibited broad-band Pauli paramagnetism. It was subsequently shown (*72*) that there is an enhancement in the susceptibility at the lowest temperature with an anomaly around 200 K (Fig. 17). The anomaly in the susceptibility at low temperatures can be attributed to paramagnetic impurities and it has been shown by Saez-Puche *et al.* (*73*) that starting with high purity oxides, the paramagnetic behavior at low temperature is suppressed although there is a tendency toward an increase in the susceptibility below 100 K. Singh *et al.* (*15*) have since found that at low temperatures, there is a marked increase in the resistivity with $\rho(12\text{ K})/\rho(300\text{ K}) \approx 10^2$. Careful magnetic susceptibility studies show that above 200 K, the susceptibility obeys a Curie law with a μ_{eff} corresponding to the contribution from about 16% of Cu^{2+} ions. At low temperatures, point by point calculation of μ_{eff} (assuming a Curie law) shows a linear decrease in the concentration of paramagnetic Cu^{2+} ions with decreasing temperature. Such a behavior seems to be consistent with the disproportionation of Cu^{2+} to Cu^{1+} and Cu^{3+} as mentioned earlier (*15*) and the formation of charge-density waves. The two B–O_I distances in the O (or O') structure of La_2CuO_4 would be consistent with orbital or-

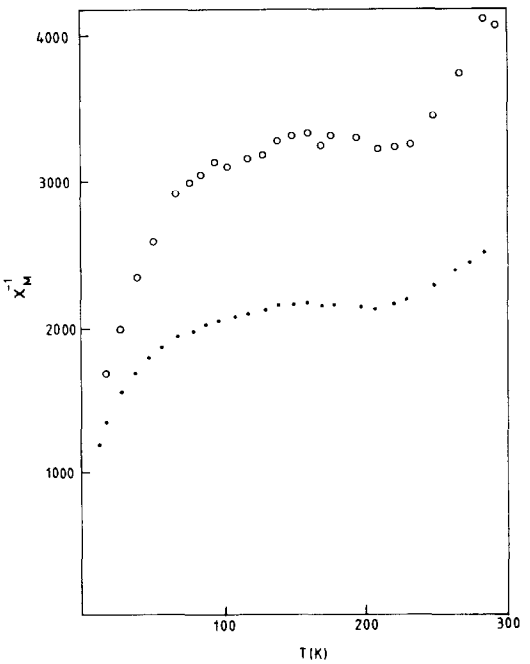

FIG. 17. χ_M^{-1} vs T plot of La_2CuO_4 at 4000 G (dotted curve); after subtraction of the contribution from the ferromagnetic component (line of circles) (from Ref. (*15*)).

dering of the type shown in Fig. 7c and it is interesting to speculate on the consequences of such ordering.

There are several intriguing features associated with Cu^{2+} ions in such oxides which are not readily understood. A comparison of the high-temperature susceptibilities of the oxides in the series $La_2Ni_{1-x}Cu_xO_4$ and $La_{2-2x}Sr_{2x}Ni_{1-x}Ti_xO_4$ shows that there is no contribution to the magnetic susceptibility at high temperatures from Cu^{2+} ions (*15*). It has been observed that Cu^{2+} ions do not contribute to the susceptibility of Ln_2CuO_4 compounds (Ln = rare earth) at low temperatures and this has been taken to indicate antiferromagnetic ordering (*72–74*).

It is extremely difficult to prepare stoichiometric La_2CoO_4. Magnetic susceptibility of $La_2CoO_{4.04}$ measured in this laboratory (*75*) shows a broad maximum around 500 K and a sharp maximum around 400 K. DSC studies show a large number of the phase transitions in this temperature region. The results have been interpreted in terms of two-dimensional magnetic ordering with the onset of three-dimensional order at low temperatures. Further work on stoichiometric samples of La_2CoO_4 is necessary to establish the magnetic behavior of this oxide.

4.4. Ferromagnetic oxides. One of the earliest oxides to be studied was $LaSr_3Mn_2O_8$ and measurements on this oxide were reported in the same paper (*76*) dealing with the low-dimensional magnetic susceptibility behaviour of K_2NiF_4. The peculiarity of $LaSr_3Mn_2O_8$ is that although the high-temperature behavior is typical of ferromagnets (the susceptibility showing a Curie–Weiss plot with a high negative values of θ), there is no spontaneous magnetization at low temperatures. This has been attributed (*77*) to the presence of small superparamagnetic clusters due to the absence of ordering of Mn^{3+} and Mn^{4+} ions (since only Mn^{3+}–O–Mn^{4+} interactions are ferromagnetic). However, the corresponding cobalt analog $LaSr_3Co_2O_8$ is a true ferromagnet with a well-defined Curie temperature (*75*). In this oxide, Co^{3+} ions could have the intermediate-spin configuration ($t_{2g}^5e_g^1$) while the Co^{4+} ions are in the low-spin configuration (t_{2g}^5). Co^{3+}–O–Co^{4+} would then be a Zener double exchange pair since the transfer of an electron from intermediate-spin Co^{3+} to low-spin Co^{4+} would have the initial and final state degenerate. Although this oxide is semiconducting, changes in the electron transport properties observed at the Curie temperature (E_a decreases below T_c) is consistent with a double exchange mechanism. Such changes in transport properties at T_c have not been observed in the corresponding three-dimensional perovskite compound $LaSrCo_2O_6$. The μ_{eff} value calculated from the χ_M^{-1} vs T plot (Fig. 18) above the Curie temperature also supports the existence of intermediate-spin Co^{3+} and low-spin Co^{4+}. At high temperatures (Fig. 18), the χ_M^{-1} vs T plot shows a Curie behavior with the μ_{eff} corresponding to high-spin Co^{3+} ions, and low-spin Co^{4+} ions. This could be associated with a low-spin to high-spin transition. It should be mentioned that the nature of the χ_M^{-1} vs T plot is similar to that predicted by Anderson and Hasegawa (*78*) for double exchange systems.

$LaSrMnO_4$ has been reported to be ferro-

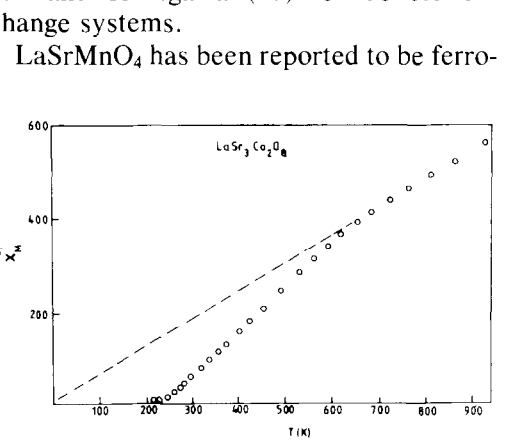

FIG. 18. χ_M^{-1} vs T plot of $LaSr_3Co_2O_8$ above 300 K.

magnetic (*79*). The electronic configuration of Mn^{3+} being the same as that of Cr^{2+}, we would expect ferromagnetism in $LaSrMnO_4$ by analogy with halides of the formula A_2CrX_4 which are transparent ferromagnets (*80*). Ferromagnetic $LaSrMnO_4$ is reported to have a tetragonal structure with a small c/a ratio while the A_2CrX_4 compounds are orthorhombic with unequal Cr–X distances in the basal plane indicative of antiferrodistortive ordering of CrX_6 octahedra. Recently, stoichiometric $LaSrMnO_4$ with a large c/a ratio (value) has been reported (*39*); we would expect ferrodistortive ordering of the elongated MnO_6 octahedra in such an oxide with the e_g electron in the d_{z^2} orbital. Considerations based on the Goodenough–Kanamori rules (*81*) indicate that the interaction would be ferromagnetic if the transfer of the $d^1_{z^2}$ electron is to the empty $d^0_{x^2-y^2}$ orbital. Magnetic measurements on stoichiometric $LaSrMnO_4$ have not been reported. The small c/a ratio of the earlier sample of $LaSrMnO_4$ suggests considerable oxygen excess non-stoichiometry and it is indeed known that the c/a ratio of $La_{1-x}Sr_{1+x}MnO_4$ decreases with increasing x.

Two oxides that have been recently studied in this laboratory (*15*) which show evidence for ferromagnetic interactions are $La_2Sr_2MnNiO_8$ and $La_2Sr_2MnCoO_8$ which are the two-dimensional analogs of the three-dimensional ferromagnets La_2MnNiO_6 and La_2MnCoO_6, respectively (*82, 83*). $La_2Sr_2MnNiO_8$ shows a large negative value of the Weiss constant, but is like $LaSr_3Mn_2O_8$ in that it does not show spontaneous magnetization at low temperatures. There is no ion ordering in either of these oxides. The c/a ratio of the former compound (3.27) is much less than that of stoichiometric $LaSrMnO_4$ (*39*), but similar to that of $LaSrNiO_4$ (*33*). This suggests that the electronic configurations of the Mn and Ni ions are $t^3_{2g}d^1_{x^2-y^2}$ and $t^6_{2g}d^1_{x^2-y^2}$, respectively, the d_{z^2} orbitals being empty in both cases. $La_2Sr_2MnCoO_8$ shows the behavior of a true ferromagnet with a well-defined Curie temperature. The c/a ratio in this compound is similar (3.28) to that of $LaSrCoO_4$ (*26, 27*), but much less than that of $LaSrMnO_4$ (*39*). Electronic configurations of the Mn^{3+} and Co^{3+} ions in this oxide appear to be $t^3_{2g}d^1_{x^2-y^2}$ and $t^5_{2g}d^1_{z^2}$, respectively. The presence of a localized d_{z^2} electron is significant. It is possible that the presence of a localized d_{z^2} electron enhances the three-dimensional B–O_I–O_I–B interlayer coupling. A mechanism that could be of relevance to compounds such as $LaSr_3Mn_2O_8$ and $La_2Sr_2MnNiO_8$ is one where the magnetic moments in the ferromagnetic state may be aligned perpendicular to the ab plane. In the absence of intralayer coupling, demagnetization effects acting on spins aligned perpendicular to a layer would be considerable.

5. Concluding Remarks

It should be clear from the above discussion that oxides with the K_2NiF_4 structure offer considerable scope for research. The anisotropic bonding coupled with strong covalency effects in these oxides could give rise to unique properties which have not been adequately investigated. For example, we are yet to understand the nature of the semiconductor–metal transition in La_2NiO_4 and other rare earth nickelates. Although many models have been suggested (*84*) to explain the transition in La_2NiO_4 (*2*), all the measurements reported hitherto are on polycrystalline samples. Preliminary studies (*12*) on single crystals of La_2NiO_4 indicate that the transition occurs sharply (550 K) with about an order of magnitude jump in conductivity along the ab plane. Anisotropic magnetic susceptibility of La_2NiO_4 needs to be investigated as also the effect of Ni^{3+} ions on these properties. The structure of La_2NiO_4 itself seems to require a revision in the light of the superlattice spots

found in the diffraction patterns. Electron transport properties of single crystals of La_2CuO_4 and related rare earth compounds are yet to be investigated. The possible occurrence of two-dimensional antiferromagnetic ordering in La_2CoO_4 is worth exploring.

An interesting feature of some of the A_2BO_4 oxides is that their electrical properties are considerably different from the corresponding perovskites, even though the magnetic properties are similar. For example, $LaSr_3Co_2O_8$ is a semiconducting ferromagnet while $LaSrCo_2O_6$ is an itinerant-electron ferromagnet. The corresponding manganese compounds also show a similar behavior. Another system showing such a behavior is that of vanadium, $La_{1-x}Sr_xVO_3$ and $La_{1-x}Sr_{1+x}VO_4$, where the latter is insulating while the former is metallic for $0.3 > x > 0.05$.

None of the A_2BO_4 oxides seems to exhibit a true metallic behavior down to the lowest temperatures. Most of these oxides show activated conduction and even those phases that have been considered to be metallic (e.g., La_2CuO_4) exhibit conductivities of the order of 10 ohm^{-1} cm^{-1}. This is much less than the conductivities found in metallic oxides of perovskite structure (e.g., La NiO_3 or $LaSrCo_2O_6$ with σ of $\sim 10^3$ ohm^{-1} cm^{-1}). It is not clear whether the absence of true metallic conductivity in A_2BO_4 oxides has something to do with localization in two dimensions (*85, 86*).

In systems where the electrical properties are determined by the concentration of the component ions, the A_2BO_4 system shows an unusual concentration dependence of resistivity. For example, delocalization of e_g electrons is found in systems like $LaSrAl_{1-x}Ni_xO_4$ when $x > 0.6$. In perovskite systems such as $La_{1-x}Sr_xCoO_3$ and $LaFe_{1-x}Ni_xO_3$, the oxides become metallic when $x = 0.25$–0.30. It is interesting to ponder whether such concentration limits are related to percolation limits in two-dimensional and cubic systems.

Some of the well-known ferroelectric materials are perovskite oxides. No ferroelectric oxide of K_2NiF_4 structure has been reported until now; similarly, other ferroic properties (*87*) are yet to be explored.

Acknowledgments

The authors thank the Department of Science and Technology, Government of India and the University Grants Commission for support of this research.

References

1. R. J. Birgeneau, H. J. Guggenheim, and G. Shirane, *Phys. Rev. B* **1,** 2211 (1970).
2. P. Ganguly and C. N. R. Rao, *Mater. Res. Bull.* **8,** 405 (1973).
3. P. Poix, *J. Solid State Chem.* **31,** 95 (1980).
4. P. Poix, *C.R. Acad. Sci. (Paris) C* **268,** 1139 (1969).
5. D. Ganguli, *J. Solid State Chem.* **30,** 353 (1979).
6. A. Rabeneau and P. Eckerlin, *Acta Crystallogr.* **11,** 304 (1958).
7. J. M. Longo and P. Raccah, *J. Solid State Chem.* **6,** 526 (1973).
8. V. U. Lehmann and H. R. Müller-Buschbaum, *Z. Anorg. Allg. Chem.* **470,** 59 (1980).
9. B. Willer and M. Dairre, *C.R. Acad. Sci. (Paris) C* **267,** 1482 (1968).
10. M. Föex, *Bull. Soc. Chim. Fr.* 109 (1961).
11. B. Grande and H. R. Müller-Buschbaum, *Z. Anorg. Allg. Chem.* **433,** 152 (1977).
12. C. N. R. Rao, D. Buttrey, N. Otsuka, P. Ganguly, H. R. Harrison, C. J. Sandberg, and J. M. Honig, *J. Solid State Chem.* **51,** 266 (1984).
13. R. Berjoan, J. P. Coutures, G. Le Flem, and S. Saux, *J. Solid State Chem.* **42,** 75 (1982), and references therein.
14. B. Grande, H. R. Müller-Buschbaum, and M. Schweizer, *Z. Anorg. Allg. Chem.* **428,** 120 (1977).
15. K. K. Singh, P. Ganguly, and J. B. Goodenough, *J. Solid State Chem.*, in press; also see K. K. Singh, Ph.D. thesis, Indian Institute of Science, Bangalore, India (1983).
16. R. D. Shannon, *Acta Crystallogr. Sect. A* **32,** 751 (1976).
17. H. R. Müller-Buschbaum and W. Wollschlager, *Z. Anorg. Allg. Chem.* **414,** 76 (1975).
18. H. R. Müller-Buschbaum, *Angew. Chem. (English transl.)* **16,** 674 (1977).
19. K. Knox, *J. Chem. Phys.* **30,** 991 (1959).

20. K. K. SINGH, P. GANGULY, AND C. N. R. RAO, *Mater. Res. Bull.* **17,** 493 (1982).
21. V. R. HAEGELE AND D. BABEL, *Z. Anorg. Allg. Chem.* **409,** 11 (1974).
22. D. REINEN AND C. FRIEBEL, *Struct. Bonding* **37,** 1 (1979).
23. J. P. OUDALOV, A. DAOUDI, J. C. JOUBERT, G. LE FLEM, AND P. HAGENMULLER, *Bull. Soc. Chim. Fr.* 3408 (1970).
24. L. FOURNES, N. KINOMURA, AND F. MENIL, *C.R. Acad. Sci. (Paris) C* **291,** 235 (1980).
25. G. DEMAZEAU, M. POUCHARD, M. THOMAS, J. F. COLOMBET, J. C. GRENIER, L. FOURNES, J. L. SOUBEYROUX, AND P. HAGENMULLER, *Mater. Res. Bull.* **15,** 451 (1980).
26. G. DEMAZEAU, P. COURBIN, G. LE FLEM, M. POUCHARD, P. HAGENMULLER, J. L. SOUBEYROUX, I. G. MAIN, AND G. A. ROBINS, *Nouv. J. Chim.* **3,** 171 (1979).
27. G. A. ROBINS, M. F. THOMAS, J. D. RUSH, G. DEMAZEAU, AND I. G. MAIN, *J. Phys. C* **15,** 233 (1982).
28. G. DEMAZEAU, M. POUCHARD, N. CHEVREAU, M. THOMAS, F. MENIL, AND P. HAGENMULLER, *Mater. Res. Bull.* **16,** 689 (1981).
29. G. DEMAZEAU, J. L. MARTY, M. POUCHARD, T. ROJO, J. M. DANCE, AND P. HAGENMULLER, *Mater. Res. Bull.* **16,** 47 (1981).
30. H. P. ROOKSBY, *Acta Crystallogr.* **1,** 266 (1948).
31. M. M. J. FAVA, Y. OUDALOV, J. M. REAU, G. LE FLEM, AND P. HAGENMULLER, *C.R. Acad. Sci. (Paris) C* **274,** 183 (1972).
32. R. D. SHANNON AND C. T. PREWITT, *Acta Crystallogr. Sect. B* **25,** 925 (1969).
33. G. DEMAZEAU, M. POUCHARD, AND P. HAGENMULLER, *J. Solid State Chem.* **18,** 159 (1976).
34. J. C. JOUBERT, A. COLLOMB, D. ELMALEH, G. LE FLEM, A. DAOUDI, AND G. OLLIVER, *J. Solid State Chem.* **2,** 343 (1970).
35. J. B. GOODENOUGH AND J. M. LONGO, "Landolt-Bornstein" (K. H. Hellwege, Ed.), Group III/4a, p. 126, Springer-Verlag, Berlin (1970).
36. S. NOMURA, "Landolt-Bornstein" (K. H. Hellwege and A. M. Hellwege, Eds.), Group III/12a, p. 425, Springer-Verlag, Berlin (1978).
37. D. S. MCCLURE, *J. Phys. Chem. Solids* **3,** 311 (1957).
38. J. A. DUFFY, *Struct. Bonding* **32,** 147 (1977).
39. A. BENABAD, A. DAOUDI, R. SALMON, AND G. LE FLEM, *J. Solid State Chem.* **22,** 121 (1977).
40. J. B. GOODENOUGH, G. DEMAZEAU, M. POUCHARD, AND P. HAGENMULLER, *J. Solid State Chem.* **8,** 325 (1973).
41. M. TAKANO, N. NAKANISHI, Y. TAKADA, S. NAKA, AND T. TAKADA, *Mater. Res. Bull.* **12,** 923 (1977).
42. S. N. RUDDLESDON AND P. POPPER, *Acta Crystallogr.* **10,** 538 (1957); **11,** 54 (1958).
43. J. A. BLAND, *Acta Crystallogr.* **14,** 875 (1961).
44. J. DRENNAN, C. P. TAVARES, AND B. C. H. STEELE, *Mater. Res. Bull.* **17,** 621 (1982).
45. R. J. D. TILLEY, *J. Solid State Chem.* **21,** 293 (1977).
46. R. PLUMIER, *J. Appl. Phys.* **35,** 950 (1964).
47. G. BLASSE, *J. Inorg. Nucl. Chem.* **27,** 2683 (1965).
48. J. F. ACKERMANN, *Mater. Res. Bull.* **14,** 487 (1979).
49. J. S. GRIFFITHS, *Mol. Phys.* **8,** 213, 217 (1964).
50. M. S. HADDED, M. W. LYNCH, W. D. FEDERER, AND D. N. HENDRICKSON, *Inorg. Chem.* **20,** 123, 131 (1981).
51. J. T. CASTNER, G. S. NEWELL, W. C. HOLTON, AND C. P. SLICHTER, *J. Chem. Phys.* **32,** 668 (1960).
52. R. MOHAN RAM, K. K. SINGH, W. H. MADHUSUDHAN, P. GANGULY, AND C. N. R. RAO, *Mater. Res. Bull.* **18,** 703 (1983).
53. G. BLASSE, *J. Inorg. Nucl. Chem.* **30,** 656 (1968).
54. J. L. SOUBEYROUX, P. COURBIN, L. FORUNES, D. FRUCHART, AND G. LE FLEM, *J. Solid State Chem.* **31,** 313 (1980).
55. J. T. LEWANDOWSKI, J. M. LONGO, AND R. A. MCCAULEY, *Amer. Ceram. Soc. Bull.* **61,** 333 (1982).
56. K. POEPPELMEIER, M. E. LEONWICZ, AND J. M. LONGO, *J. Solid State Chem.* **44,** 89 (1982).
57. K. VIDYASAGAR, J. GOPALAKRISHNAN, AND C. N. R. RAO, *Inorg. Chem.*, in press.
58. W. H. MADHUSUDHAN, K. JAGANNATHAN, P. GANGULY, AND C. N. R. RAO, *J. Chem. Soc. Dalton Trans.* 1397 (1980).
59. S. RAMASESHA, T. V. RAMAKRISHNAN, AND C. N. R. RAO, *J. Phys. C* **12,** 1307 (1979).
60. G. BLASSE, *J. Appl. Phys.* **36,** 879 (1965).
61. G. DEMAZEAU, J. L. MARTY, B. BUFFAT, J. M. DANCE, N. POUCHARD, P. DORDOR, AND B. CHEVALIER, *Mater. Res. Bull.* **17,** 37 (1982).
62. D. E. COX, G. SHIRANE, R. J. BIRGENEAU, AND J. B. MACCHESNEY, *Phys. Rev.* **188,** 930 (1969).
63. J. C. BOULOUX, J. L. SOUBEYROUX, M. PERRIN, AND G. LE FLEM, *J. Solid State Chem.* **38,** 34 (1981).
64. G. LE FLEM, G. DEMAZEAU, AND P. HAGENMULLER, *J. Solid State Chem.* **44,** 82 (1982).
65. G. OLLIVER, These de Doctorates Sciences Physiques, Univ. Scientifique et Medicale, Grenoble (1973).
66. J. B. GOODENOUGH, *Progr. Solid State Chem.* **5,** 145 (1972); "Solid State Chemistry," (C. N. R. Rao, Ed.), Dekker, New York (1973).
67. M. SHIMADA AND M. KOIZUMI, *Mater. Res. Bull.* **11,** 1237 (1976).

68. B. K. SHANTE AND S. KIRKPATRICK, *Advan. Phys.* **20,** 325 (1971).
69. W. M. WALSH, R. J. BIRGENEAU, L. W. RUPP, AND H. J. GUGGENHEIM, *Phys. Rev. B* **20,** 4645 (1979).
70. G. A. SMOLENSKII, V. N. YUDIN, AND E. SHER, *Sov. Phys. Solid State* **4,** 2452 (1962).
71. G. A. SMOLENSKII, V. A. BOKOV, S. A. KIZAEV, E. I. MAL'TEEV, G. M. NEDHIR, V. P. P. PLAKNTY, A. G. TUTOV, AND V. N. YUDIN, "Proceedings International Conference on Magnetism, Nottingham, 1964," p. 354, Inst. Phys. and Phys. Soc. London (1965).
72. P. GANAGULY, S. KOLLALI, C. N. R. RAO, AND S. KERN, *Magn. Lett.* **1,** 107 (1980).
73. R. SAEZ-PUCHE, M. NORTON, AND W. S. GLAUNSINGER, *Mater. Res. Bull.* **17,** 1523 (1982).
74. R. SAEZ-PUCHE, M. NORTON, AND W. S. GLAUNSINGER, *Mater. Res. Bull.* **17,** 1539 (1982).
75. P. GANGULY AND S. RAMASESHA, *Magn. Lett.* **1,** 131 (1980).
76. K. G. SRIVATSAVA, *Phys. Lett.* **4,** 55 (1963).
77. J. C. BOULOUX, J. L. SOUBEYROUX, A. DAOUDI, AND G. LE FLEM, *Mater. Res. Bull.* **16,** 855 (1981).
78. P. W. ANDERSON AND H. HASEGAWA, *Phys. Rev.* **100,** 675 (1955).
79. J. B. MACCHESNEY, J. F. POTTER, AND R. C. SHERWOOD, *J. Appl. Phys.* **40,** 1243 (1969).
80. P. DAY, *Acc. Chem. Res.* **12,** 236 (1973), and references therein.
81. J. B. GOODENOUGH, "Magnetism and the Chemical Bond," Wiley–Interscience, New York (1963).
82. J. B. GOODENOUGH, A. WOLD, R. J. ARNOTT, AND N. MENYUK, *Phys. Rev.* **124,** 373 (1961).
83. N. Y. VASANTHACHARYA, K. K. SINGH, AND P. GANGULY, *Rev. Chim. Miner.* **18,** 333 (1981), and references therein.
84. J. B. GOODENOUGH AND S. RAMASESHA, *Mater. Res. Bull.* **17,** 383 (1982).
85. E. ABRAHAM, P. W. ANDERSON, D. C. LICCARDELLO, AND T. V. RAMAKRISHNAN, *Phys. Rev. Lett.* **42,** 673 (1979).
86. E. ABRAHAM AND T. V. RAMAKRISHNAN, *J. Non-Cryst. Solids* **35,** 15 (1980); *Philos. Mag.* [*Part*] *B* **42,** 827 (1980).
87. R. E. NEWNHAM AND L. E. CROSS, *in* "Preparation and Characterization of Materials" (J. M. Honig and C. N. R. Rao, Eds.), Academic Press, New York (1981).